

# The US 2000-2002 Market Descent: How Much Longer and Deeper?

Didier Sornette <sup>1,2,3</sup> and Wei-Xing Zhou <sup>1</sup>

1. Institute of Geophysics and Planetary Physics, University of California, Los Angeles, CA 90095
2. Department of Earth and Space Sciences, University of California, Los Angeles, CA 90095
3. Laboratoire de Physique de la Matière Condensée, CNRS UMR 6622 and Université de Nice-Sophia Antipolis, 06108 Nice Cedex 2, France

## Abstract

A remarkable similarity in the behavior of the US S&P500 index from 1996 to August 2002 and of the Japanese Nikkei index from 1985 to 1992 (11 years shift) is presented, with particular emphasis on the structure of the bearish phases. Extending a previous analysis of Johansen and Sornette [1999, 2000] on the Nikkei index “anti-bubble” based on a theory of cooperative herding and imitation working both in bullish as well as in bearish regimes, we demonstrate the existence of a clear signature of herding in the decay of the S&P500 index since August 2000 with high statistical significance, in the form of strong log-periodic components. We offer a detailed analysis of what could be the future evolution of the S&P500 index over the next two years, according to three versions of the theory: we expect an overall continuation of the bearish phase, punctuated by local rallies; we predict an overall increasing market until the end of the year 2002 or at the beginning of 2003 (first quarter); we predict a strong following descent (with maybe one or two severe up and downs in the middle) which stops during the first semester of 2004. After this strong minimum, the market is expected to recover. Beyond, our prediction horizon is made fuzzy by the possible effect of additional nonlinear collective effects and of a real departure from the anti-bubble regime. The similarities between the two stock market indices may reflect deeper similarities between the fundamentals of two economies which both went through over-valuation with strong speculative phases preceding the transition to bearish phases characterized by a surprising number of bad surprises (bad loans for Japan and accounting frauds for the US) sapping investors’ confidence.

## 1 Introduction

Financial crashes have been proposed to be critical phenomena in the statistical physics sense of critical phase transitions (see [23, 10, 16, 9, 22, 20] and references therein). Two hallmarks of criticality have been documented: (i) super-exponential power law acceleration of the price towards a “critical” time  $t_c$  corresponding to the end of the speculative bubble and (ii) log-periodic modulations accelerating according to a geometric series signaling a discrete hierarchy of time scales.

Imitation between investors and their herding behavior not only lead to speculative bubbles with accelerating overvaluations of financial markets possibly followed by crashes, but also to “anti-bubbles” with decelerating market devaluations following market peaks. There is thus a certain degree of symmetry between the speculative behavior of the “bull” and “bear” market regimes. This degree of symmetry, after the critical time  $t_c$ , corresponds to the existence of “anti-bubbles.”

characterized by a power law decrease of the price (or of the logarithm of the price) as a function of time  $t > t_c$ , down from a maximum at  $t_c$  (which is the beginning of the anti-bubble) and by decelerating/expanding log-periodic oscillations [11]. The classic example of such an anti-bubble is the long-term depression of the Japanese index, the Nikkei, that has decreased along a downward path marked by a succession of up and downs since its all-time high of 31 Dec. 1989. Another good example is found for the gold future prices after 1980, after its all-time high. The Russian market prior to and after its speculative peak in 1997 also constitutes a remarkable example where both bubble and anti-bubble structures appear simultaneously for the same  $t_c$ . This is however a rather rare occurrence, probably because accelerating markets with log-periodicity often end-up in a crash, a market rupture that thus breaks down the symmetry ( $t_c - t$  for  $t < t_c$  into  $t - t_c$  for  $t > t_c$ ). Herding behavior can occur and progressively weaken from a maximum in “bearish” (decreasing) market phases, even if the preceding “bullish” phase ending at  $t_c$  was not characterized by an imitation run-away. The symmetry is thus statistical or global in general and holds in the ensemble rather than for each single case individually.

In [11, 12], the decrease of the Nikkei index has been analyzed in details, starting from 1 Jan. 1990, using three increasingly complex formulas, corresponding to the three successive orders of a Landau expansion around 0 of the logarithm of the price:  $\frac{d \ln F(x)}{d \ln x} = \alpha F(x) + \dots$ , where in general the coefficients may be complex. The first-order expression based on discrete scale invariance [19] of stock indices reads:

$$\ln p(t) \approx A_1 + B_1 \tau^\alpha + C_1 \tau^\alpha \cos [\omega \ln(\tau) + \phi_1], \quad (1)$$

where

$$\tau = t - t_c, \quad (2)$$

where  $t_c$  is the time of the beginning of the anti-bubble. The inclusion of a non-linear quadratic term in the Landau expansion leads to the second-order log-periodic formula [21]

$$\ln p(t) \approx A_2 + \frac{\tau^\alpha}{\sqrt{1 + \left(\frac{\tau}{\Delta_t}\right)^{2\alpha}}} \left\{ B_2 + C_2 \cos \left[ \omega \ln(\tau) + \frac{\Delta_\omega}{2\alpha} \ln \left( 1 + \left(\frac{\tau}{\Delta_t}\right)^{2\alpha} \right) + \phi_2 \right] \right\}. \quad (3)$$

A third-order formula has also been given in [11] which derives from the addition of a third-order term in the Landau expansion. We do not write this formula explicitly here as we shall not need it for the present analysis. Equation (3) describes a transition from an angular log-frequency  $\omega$  (for  $\tau < \Delta_t$ ) to a different angular log-frequency  $\omega + \Delta_\omega$  (for  $\Delta_t < \tau$ ). Note that expression (3) reduces to equation (1) in the limit  $\Delta_t \rightarrow +\infty$ . Using these three formulas, a prediction was published in January 1999 on the behavior of the Japanese stock market in the following two years [11], that have been remarkably successful [12].

The present situation of Japan does not seem any more very different from that of the US after the burst of the “new economy” bubble in March-April 2000 [13] (paralleling the end of the Japanese bubble in January 1990) and the cascade of discoveries, not yet fully unveiled in their full extent, of creative accounting of companies striving to look good in the eyes of analysts rather than to build strong fundamentals (paralleling the discovery of a surprising amount of bad loans held by Japanese banks). This remark takes a forceful meaning when looking at Fig. 1, which compares the behavior of the Japanese Nikkei index and of the US S&P500 index under a time shift of 11 years. The three fits of the Nikkei index, shown in Fig. 1 as undulating lines, use the three mathematical expressions discussed above. The dashed line is the simple log-periodic formula (1); the dotted line is the improved nonlinear log-periodic formula (3) developed in [21] and also used for the

October 1929 and October 1987 crashes over 8 years of data; the continuous line is the extension of the previous nonlinear log-periodic formula to the third-order Landau expansion developed in Ref. [11]. This last more sophisticated mathematical formula predicts the transition from an angular log-frequency  $\omega$  (for  $\tau < \Delta_t$ ) to another angular log-frequency  $\omega + \Delta_\omega$  for  $\Delta_t < \tau < \Delta'_t$  and to a third angular log-frequency  $\omega + \Delta_\omega + \Delta'_\omega$  (for  $\Delta'_t < \tau$ ).

In the next section, we use the insight provided by the theory of critical herding [23, 10, 16, 9, 22, 20] to analyze the S&P500 2000-2002 antibubble. We perform a battery of tests, starting with parametric fits of the index with two of the above log-periodic power law formulas, followed by the so-called Shank's transformation applied to characteristic times. We then present two spectral analysis, the Lomb periodogram applied to the parametrically detrended index and the non-parametric  $(H, q)$ -analysis of fractal signals. These different approaches complement each other and confirm the remarkably strong presence of log-periodic structures. We also detect a significant second-order harmonic which provides a statistically significant improvement of the description of the data by the theory, as tested using the statistical theory of nested hypotheses. Section 3 offers an analysis of what could be the future evolution of the S&P500 index over the next two years by comparing the predictions of three formulas. The predictions are found to be robust and consistent. We conclude by speculating in section 4 on possible consequences as well as projections further ahead.

## 2 Analysis of the S&P500 2000-2002 antibubble

### 2.1 Theoretical foundations

The analysis presented below relies on a general theory of financial crashes and of stock market instabilities developed in a series of works (see [23, 10, 16, 9, 22, 20] and references therein). The main ingredient of the theory is the existence of positive feedbacks in stock markets as well as in the economy. Positive feedbacks, i.e., self-reinforcement, refer to the fact that, conditioned on the observation that the market has recently moved up (respectively down), this makes it more probable to keep it moving up (respectively down), so that a large cumulative move may ensue. The concept of “positive feedbacks” has a long history in economics and is related to the idea of “increasing returns”— which says that goods become cheaper the more of them are produced (and the closely related idea that some products, like fax machines, become more useful the more people use them). “Positive feedback” is the opposite of “negative feedback”, a concept well-known for instance in population dynamics: the larger the population of rabbits in a valley, the less they have grass per rabbit. If the population grows too much, they will eventually starve, slowing down their reproduction rate which thus reduces their population at a later time. Thus negative feedback means that the higher the population, the slower the growth rate, leading to a spontaneous regulation of the population size; negative feedbacks thus tend to regulate growth towards an equilibrium. In contrast, positive feedback asserts that the higher (respectively lower) the price or the price return in the recent past, the higher (respectively lower) will be the price growth in the future. Positive feedbacks, when unchecked, can produce runaways until the deviation from equilibrium is so large that other effects can be abruptly triggered and lead to rupture or crashes. Alternatively, it can give prolonged depressive bearish markets.

There are many mechanisms leading to positive feedbacks including hedging derivatives, insurance portfolios, investors' over-confidence, imitative behavior and herding between investors. Such positive feedbacks provide the fuel for the development of speculative bubbles as well as anti-bubbles [11, 12], by the mechanism of cooperativity, that is, the interactions and imitation between traders may lead to collective behaviors similar to crowd phenomena. Different types of collective

regimes are separated by so-called critical points which, in physics, are widely considered to be one of the most interesting properties of complex systems. A system goes critical when local influences propagate over long distances and the average state of the system becomes exquisitely sensitive to a small perturbation, *i.e.* different parts of the system become highly correlated. Another characteristic is that critical systems are self-similar across scales: at the critical point, an ocean of traders who are mostly bearish may have within it several continents of traders who are mostly bullish, each of which in turns surrounds seas of bearish traders with islands of bullish traders; the progression continues all the way down to the smallest possible scale: a single trader [25]. Intuitively speaking, critical self-similarity is why local imitation cascades through the scales into global coordination. Critical points are described in mathematical parlance as singularities associated with bifurcation and catastrophe theory. At critical points, scale invariance holds and its signature is the power law behavior of observables.

The last ingredient of the model is to recognize that the stock market is made of actors which differ in size by many orders of magnitudes ranging from individuals to gigantic professional investors, such as pension funds. Furthermore, structures at even higher levels, such as currency influence spheres (US\$, Euro, YEN ...), exist and with the current globalization and de-regulation of the market one may argue that structures on the largest possible scale, *i.e.*, the world economy, are beginning to form. This means that the structure of the financial markets have features which resembles that of hierarchical systems with “traders” on all levels of the market. Of course, this does not imply that any strict hierarchical structure of the stock market exists, but there are numerous examples of qualitatively hierarchical structures in society. Models of imitative interactions on hierarchical structures predict that the power law behavior can be decorated by so-called log-periodic corrections. Indeed, through the existence of preferred scales in a discrete hierarchy, or a discrete cascade of instabilities [19] or the existence of a competition between positive and negative nonlinear feedbacks [7], the scale invariance characterizing critical points may be partially broken into a discrete scale invariance, that is, the observable is invariant with respect to changes of scales which are integer powers of a fundamental scaling ratio  $\lambda$ . It is easy to show that log-periodicity as given by the term  $C_1 \tau^\alpha \cos[\omega \ln(\tau) + \phi_1]$  of expression (1) is the signature of discrete scale invariance: the term  $\cos[\omega \ln(\tau) + \phi_1]$  reproduces itself each time  $\ln \tau$  changed by  $2\pi/\omega$ , that is, each time  $\tau$  is multiplied by  $\lambda = \exp[2\pi/\omega]$ . This theory predicts robust and universal signatures of speculative phases of financial markets, both in accelerating bubbles as well as in decelerating anti-bubbles. These precursory patterns have been documented for essentially all crashes on developed as well as emergent stock markets, on currency markets, on company stocks, etc.

## 2.2 Log-periodic fits

We use equations (1) and (3) to fit the logarithm of the S&P500 index over an interval starting at time  $t_{\text{start}}$  and ending at Aug. 24, 2002. The justification of the use of the logarithm of the price is presented in [10]. The choice of  $t_{\text{start}}$  is not completely obvious. It is clear that it should be close to the peak of the S&P500 index in 2000 but cannot be expected to be exactly coincident with the time of the peak due to finite-size and other effects spoiling the validity of the log-periodic power law. We address this problem in two ways. First, we scan  $t_{\text{start}}$  and select 10 time series, starting respectively at  $t_{\text{start}} = 1\text{st March } 2000, 1\text{st April } 2000, \dots, 1\text{st December } 2000$ . The comparison of the fits obtained for these 10 time series will give a sense of their sensitivity with respect to  $t_{\text{start}}$ . Second, we notice that we can generalize the definition of  $\tau$  given by (2) into

$$\tau = |t - t_c|. \quad (4)$$

While definition (2) together with the logarithmic as well as power law singularities associated with formulas (1) and (3) imposes that  $t_c < t_{\text{start}}$  for an anti-bubble, the definition (4) allows for the critical time  $t_c$  to lie anywhere within the time series. In that case, the part of the time series for  $t < t_c$  corresponds to an accelerating “bubble” phase while the part  $t > t_c$  corresponds to a decelerating “anti-bubble” phase. Definition (4) has thus the advantage of introducing a degree of flexibility in the search space for  $t_c$  without much additional cost. In particular, it allows us to avoid a thorough scanning of  $t_{\text{start}}$  since the value of  $t_c$  obtained with this procedure is automatically adjusted without constraint.

There are two potential problems associate with this new procedure (4). First, it assumes that the anti-bubble is always associated with a bubble which, in addition, has the same  $t_c$ . Second, it assumes that the bubble and anti-bubble are exactly symmetric around  $t_c$ , that is, the same parameters characterize the index evolution for  $t < t_c$  and for  $t > t_c$ . For the cases relevant to the present study, these two problems are quite minor and can be neglected because  $t_c$  is always found close to  $t_{\text{start}}$  (within the time series for  $t_{\text{start}}$  prior to August 2000 and anterior to the time series otherwise). Our comparison with fits using (2) shows that the new procedure provides significantly better and more stable fits, with in particular a value of  $t_c$  very weakly sensitive to  $t_{\text{start}}$ . The parameters of the fits with the first-order formula using (2) or (4) are presented in Table 1, using subscripts 0 and 1 respectively. The fits with the first-order formula (1) with the definition (2) are unstable, are quite sensitive to  $t_{\text{start}}$  and have on average much larger values of their residuals  $\chi$  ( $\chi_0 > \chi_1$ ). Comparing parameters with subscripts 1 and 2, one can see that applying the symmetry condition (4) improves the quality of fit remarkably. We stress however that this improvement (4) is not crucial and our results reported below remain robust with the definition (2). It would also be quite easy to relax the constraints of (4) by replacing  $\tau = |t - t_c|$  by an asymmetric function allowing in addition for a plateau or time lag. Since this would involve additional and poorly constrained additional parameters, we do not pursue this possibility here.

The results of the fits of the logarithm of the S&P 500 index from  $t_{\text{start}}$  to August, 24, 2002 with Eqs. (1) and (3) using the improved scheme (4) are presented in figure 2 and in Table 1 under the subscripts 1 and 2 respectively. The ten oscillating curves correspond to the ten best fits, one for each of the 10 chosen values of  $t_{\text{start}}$  from March to December 2000. Over the approximately two years period available for the S&P500 anti-bubble, we find that the two formulas give essentially the same results and the same predictions for the following year. This is reflected quantitatively by the facts that  $\chi_1 \approx \chi_2$  and that the parameters  $\Delta_t$ 's are extremely large, in which case expression (3) reduces to equation (1) in the limit  $\Delta_t \rightarrow +\infty$ . The top (respectively bottom) panel corresponds to using equation (1) (respectively (3)). The curves are shown as continuous line in their fitting interval and as dotted line in their extrapolation to the future. Note the very robust nature of the solutions obtained for the ten choices of  $t_{\text{start}}$ , which essentially all agree in their parameters and in their prediction of the future evolution.

To sum up, varying the starting date  $t_{\text{start}}$  of the fitted time window over a 10-month period and using two formulas, we confirm that a single log-periodic power law describes very well the S&P500 anti-bubble since around mid-2000. According to the values of  $t_{c,1}$  listed in Table 1, the critical  $t_c$  is around 09-Aug-2000. This is consistent with the fact that the fit residuals obtained with  $t_{\text{start}} = 01\text{-Mar-}2000, 01\text{-Apr-}2000, 01\text{-Oct-}2000, 01\text{-Nov-}2000$  and  $01\text{-Dec-}2000$  are significantly larger ( $\chi_1 > 3.3$ ) than the residuals for the other values of  $t_{\text{start}}$ . It is natural that fits with  $t_{\text{start}}$  close to  $t_c$  have smaller fit residuals. The fits with  $t_{\text{start}} = 01\text{-May-}2000, 01\text{-Jun-}2000, 01\text{-Jul-}2000, 01\text{-Aug-}2000$  and  $01\text{-Sep-}2000$  indeed exhibit smaller residuals. This conclusion is also supported by the values of  $\omega$  and of  $\alpha$  which are basically constant for these five starting dates. Combining all the information shown in Table 1, we have the critical time  $t_c = 09\text{-Aug-}2000 \pm 5$  days, the angular

log-frequency  $\omega = 10.30 \pm 0.17$  and the exponent  $\alpha = 0.69 \pm 0.02$ . The fits with the second-order formula (3) gives similar results.

### 2.3 Analysis using the Shank's transformation on a hierarchy of characteristic times

The fundamental idea behind the appearance of log-periodicity is the existence of a hierarchy of characteristic scales. Reciprocally, any log-periodic pattern implies the existence of a hierarchy of characteristic time scales. This hierarchy of time scales is determined by the local positive maxima or minima of the function such as  $\log[p(t)]$ . For the S&P500 index anti-bubble, let us consider the times  $t_n$  at which the S&P500 index reached a local minimum. As seen in figure 2, there is a clear sequence of sharp minima. We number them from the most recent one  $t_1 = 23\text{-Jul-2002}$ ,  $t_2 = 21\text{-Sep-2001}$ ,  $t_3 = 04\text{-Apr-2001}$ ,  $t_4 = 20\text{-Dec-2000}$  up to the earliest one at  $t_5 = 12\text{-Oct-2000}$ , which is still obvious. According to the prediction of log-periodicity, the spacing between successive values of  $t_n$  approaches zero as a geometric series as  $n$  becomes large and  $t_n$  converges to  $t_c$ . We have  $t_1 - t_2 = 305$  days,  $t_2 - t_3 = 170$  days,  $t_3 - t_4 = 105$  days and  $t_4 - t_5 = 69$  days.

Specifically, log-periodicity predicts that the times  $t_n$  are organized in a geometric time series such that

$$t_n - t_c = \frac{\tau}{\lambda^n}, \quad (5)$$

where  $\tau$  sets the time unit and

$$\lambda = e^{\frac{2\pi}{\omega}} \quad (6)$$

is the preferred scaling ratio. The relation (5) leads to

$$\frac{t_n - t_c}{t_{n+1} - t_c} = \frac{t_n - t_{n+1}}{t_{n+1} - t_{n+2}} = \lambda, \quad (7)$$

which is a signature of the discrete self-similarity of the log-periodic oscillations. Using the previously determined dates  $t_1, \dots, t_5$ , we obtain

$$\frac{t_1 - t_2}{t_2 - t_3} = 1.79, \quad (8)$$

$$\frac{t_2 - t_3}{t_3 - t_4} = 1.62, \quad (9)$$

$$\frac{t_3 - t_4}{t_4 - t_5} = 1.52. \quad (10)$$

These three values given by (8,9,10) are compatible but smaller than the value of  $\lambda = 1.9 \pm 0.1$  deduced from the log-periodic fits shown in Table 1. Note that, according to the theory, the hierarchy of scales  $t_c - t_n$  are not universal but depend upon the specification of the system. What is expected to be universal are the ratios  $\frac{t_{n+1} - t_c}{t_n - t_c} = \lambda$ .

From three successive observed values of  $t_n$ , say  $t_n, t_{n+1}$  and  $t_{n+2}$ , we can obtain an estimation of the critical time by the following formula

$$t_c = \frac{t_{n+1}^2 - t_{n+2}t_n}{2t_{n+1} - t_n - t_{n+2}}. \quad (11)$$

This relation applies the so-called Shanks transformation [1] to accelerate the convergence of series. In the case of an exact geometrical series, three terms are enough to converge exactly to the asymptotic value  $t_c$ . Notice that this relation is invariant with respect to an arbitrary translation in

time. Applying (11) with  $t_1, t_2, t_3$  gives  $t_c = 02\text{-Sep-2000}$ . Applying (11) with  $t_2, t_3, t_4$  gives  $t_c = 03\text{-Jul-2000}$ . Applying (11) with  $t_3, t_4, t_5$  gives  $t_c = 01\text{-Jun-2000}$ . These back-predictions for  $t_c$  are compatible with the value of  $t_c = 09\text{-Aug-2000} \pm 5$  days given in Table 1 determined by the log-periodic fits.

In addition, the geometric structure of the time series  $t_1, t_2, \dots$  is such that the next time  $t_{n+3}$  can be obtained from the first three ones by

$$t_{n+3} = \frac{t_{n+1}^2 + t_{n+2}^2 - t_n t_{n+2} - t_{n+1} t_{n+2}}{t_{n+1} - t_n}. \quad (12)$$

Since time is measured backward as  $n$  increases, we are interested in the time  $t_0$  at which the next future minimum occurs. For this, we use formula (12) and put  $n = 0$  to get

$$t_0 = \frac{t_1^2 + t_2^2 - t_1 t_2 - t_1 t_3}{t_2 - t_3} \approx 21 \text{ Jan } 2004. \quad (13)$$

While this Shank analysis has the advantage of simplicity and of having an obvious geometrical interpretation, its weakness lies in using a geometric set of characteristic times  $\{t_n\}$  whose identification may be quite subjective. In the present case, the minima are so distinctive and sharp that there is no ambiguity. But, the use of only three characteristics dates makes more serious the sensitivity to noise and is of course bounded to lead to less precise fits and predictions than the full parametric fits reported in the previous section 2.2.

## 2.4 Spectral analysis

While the two previous analyses are suggestive, the parametric nature of the first one and the limited power of the second one requires additional tests of the reported log-periodicity. In this goal, we now turn to objective approaches for the detection of log-periodicity by applying a spectral Lomb analysis [17]. The Lomb analysis is a spectral analysis designed for unevenly sampled data which gives the same results as the standard Fourier spectral analysis. We apply this spectral analysis to two types of signals. Following [8], the first one is obtained by detrending the logarithm of the S&P500 index, using the power law (without log-periodicity) with the exponent  $\alpha$  determined from the previous fits with formula (1). The time series of the residuals of the simple power law fit should be a pure cosine of  $\ln \tau$  if log-periodicity was perfect. We also use a recently developed non-parametric approach called the  $(H, q)$ -analysis, which has been successfully applied to financial crashes [29] and critical ruptures [28] for the detection of log-periodic components.

### 2.4.1 Parametric detrending approach

We first construct the following detrended quantity which is defined using Eq. (1) by:

$$r(t) = \ln \left[ \frac{A_1 - \ln p(t)}{(t - t_c)^\alpha} \right] - \left\langle \ln \left[ \frac{A_1 - \ln p(t)}{(t - t_c)^\alpha} \right] \right\rangle, \quad (14)$$

where the bracket refers to the sample average. Table 1 shows that the values of  $A_1$  and  $\alpha$  are quite stable and approximately equal to 7.33 and 0.69 for different  $t_{\text{start}}$ . In order to investigate the impact of the different choice of  $t_c$ , we first construct  $\ln p(t) - A_1$  as a function of  $\ln(t - t_c)$  for different  $t_c$  by fixing  $A_1 = 7.33$ . We then detrend it directly by determining the exponent  $\alpha$  from a linear fit, whose residuals  $r(t)$  define the time series to be analyzed for log-periodicity.

Figure 3 shows the residual time series  $r(t)$  as a function of  $\ln(t - t_c)$  for three different critical times  $t_c$ : 15-Jul-2000 (top panel), 01-Aug-2000 (mid panel) and 15-Aug-2000 (bottom panel). The log-periodic undulations are clearly visible. We then perform the spectral Lomb analysis on these residuals. The three corresponding Lomb periodograms shown in Fig. 4 are very consistent with each other. They all exhibit an extremely strong and significant peak close to the log-frequency  $f = \omega/2\pi = 1.7$  with an amplitude larger than 140. Its harmonic shown as the downward pointing arrow is significant. As we shall discuss later in section 2.5, the existence of harmonics have been shown to be important factors for qualifying log-periodicity [27, 30]. The presence of this harmonic is thus taken as a confirmation of the presence of log-periodicity. The third peak at  $f = 2.5 - 3$  is also significant but less well-constrained. The inset of Fig. 4 magnifies the Lomb periodogram in the neighborhood of the largest peaks. The two highest Lomb peaks for  $t_c = 01\text{-Aug-2000}$  and  $t_c = 15\text{-Aug-2000}$  are significantly higher than the highest peak for  $t_c = 15\text{-Jul-2000}$ , confirming that the critical time is somewhere between 01-Aug-2000 and 15-Aug-2000 (recall that section 2.2 found  $t_c \approx 09\text{-Aug-2000} \pm 5$  days). As the number of the data points used for the Lomb analysis is the same in all analyses throughout this paper, this warrants a comparison of the Lomb peak heights for different  $t_c$ 's to establish their significance levels [26]. The log-periodic frequency of the largest peak for  $t_c = 01\text{-Aug-2000}$  is  $f = 1.71$ , corresponding to  $\omega = 2\pi f = 10.7$ , which is in reasonable agreement with the value  $\omega = 10.30 \pm 0.17$  reported in Table 1.

To further assess the sensitivity with respect to the choice of  $t_c$ , we choose 21 different  $t_c$  evenly spaced in the time interval from 15-Jul-2000 to 13-Sep-2000. For each  $t_c$ , we perform the same analysis as above and obtain the highest Lomb peak and its associated log-frequency. The results are shown in Fig. 5. The log-frequency is found to decrease with  $t_c$ . This is due to the fact that, moving the critical time forward (respectively backward), the other end of the time series will decelerate (respectively accelerate) the log-periodic oscillations. Fig. 5 confirms that the best critical time  $t_c$  falls somewhere in the first half of August 2000. The corresponding log-frequencies are  $f = 1.63 - 1.72$  ( $\omega = 10.2 - 10.7$ ), in agreement with Table 1.

It is interesting that the most relevant angular log-frequency  $\omega \approx 10$  fitted on the S&P500 index is found very close to twice the value  $\approx 5$  found previously for the Nikkei index. Actually, a small but noticeable peak at this value  $f \approx 5/2\pi \approx 0.80$  can be seen in Fig. 4, strengthening the analogy quantitatively. It may thus be surmised that both the Nikkei and the S&P500 indices are characterized by a universal discrete hierarchy of (angular) log-periodic frequencies, all harmonics of a fundamental angular log-frequency close to 5. Other systems have previously exhibited the curious fact, also observed when comparing the S&P500 to the Nikkei indices, that the higher-order harmonics may have an amplitude larger than the fundamental value [15, 27, 30], as observed for the S&P500 index.

#### 2.4.2 Non-parametric $(H, q)$ -analysis

The  $(H, q)$ -analysis [28, 29] is a generalization of the  $q$ -analysis [2, 3], which is a natural tool for the description of discretely scale invariant fractals. The  $(H, q)$ -derivative is defined as

$$D_q^H f(x) \triangleq \frac{f(x) - f(qx)}{[(1 - q)x]^H}. \quad (15)$$

The special case  $H = 1$  recovers the normal  $q$ -derivative, which itself reduces to the normal derivative in the limit  $q \rightarrow 1^-$ . There is no loss of generality by constraining  $q$  in the open interval  $(0, 1)$  [28]. We apply the  $(H, q)$ -analysis to verify non-parametrically the existence of log-periodicity by taking  $f(x) = \ln p(t)$  and  $x = t - t_c$ . The advantage of the  $(H, q)$ -analysis is that there is no need

of detrending as done in the previous section 2.4.1. Such detrending is automatically accounted for by the finite difference and the normalization by the denominator.

Fig. 6 shows the  $(H, q)$ -derivatives of the logarithm of S&P500 index as a function  $f \ln(t - t_c)$  for three choice of  $t_c$ : 15-Jul-2000 with  $H = 0$  and  $q = 0.8$  in the top panel, 02-Aug-2000 with  $H = 0.5$  and  $q = 0.7$  in the mid panel, and 16-Aug-2000 with  $H = 0.4$  and  $q = 0.7$  in the bottom panel. Each of these pairs of  $(H, q)$  is the optimal pair [28, 29] corresponding to the most significant peak among all Lomb periodograms for each  $t_c$ . The log-periodic undulations are clearly visible to the naked eyes. The Lomb periodograms of the  $(H, q)$ -derivatives shown in Fig. 6 are presented in Fig. 7. The three highest Lomb peaks are even more significant than those in Fig. 4. The inset shows the magnified Lomb peaks. The highest Lomb peak is obtained for  $t_c = 02\text{-Aug-2000}$ , which corresponds to the log-frequency  $f \approx 1.71$ .

To test the robustness of the  $(H, q)$ -analysis for the detection of log-periodicity, we scan  $H$  from  $-1$  to  $1$  with spacing  $0.1$  and  $q$  from  $0.1$  to  $0.9$  with spacing  $0.1$  for each critical  $t_c$ . Figure 8 shows the log-frequency  $f$  as a function of  $H$  and  $q$  for  $t_c = 16\text{-Aug-2000}$ . The existence of a flat plateau at  $f = 1.62 \pm 0.07$  for most of the pairs  $(H, q)$  confirm the existence of log-periodicity. The five smaller log-frequencies below the plateau correspond to the spurious values stemming from the most probable effect of noise on power laws [6] and should be discarded. The three higher log-frequencies above the plateau probably stem from the interaction between high-frequency noise and the second harmonics.

We then apply the non-parametric  $(H, q)$ -analysis to the S&P500 index for 21 different choices of the critical  $t_c$ . For each given  $t_c$ , we take the average of the Lomb periodograms for all  $21 \times 9$  pairs of  $(H, q)$ . The amplitude of the highest peak in each averaged Lomb periodogram is plotted as a function of  $t_c$  in the lower panel of Fig. 9. Their associated log-frequency shown in the upper panel of Fig. 9 with error bars is estimated from the average height of the plateaus such as the one seen in Fig. 8. This log-frequency slightly decreases with  $t_c$ . There are two clear humps in the lower panel around late July and mid August 2000. The hump around mid August is higher than the other one. The corresponding log-frequencies  $f \approx 1.60 - 1.70$  are compatible with those reported in Table 1.

## 2.5 Role of log-periodic harmonics

The spectral Lomb analyses reported above (see figures 4 and 7) as well as a the visual structure of the S&P500 time series suggest the presence of a rather strong harmonic at the angular log-frequency  $2\omega$ . The possible importance of harmonics in order to qualify log-periodicity is made also more credible by recent analyses of log-periodicity in hydrodynamic turbulence data [27, 30] which have demonstrated the important role of higher harmonics in the detection of log-periodicity.

We thus revisit the parametric log-periodic fits of section 2.2 with formula (1) using (4) to include the effect of an harmonic at the angular log-frequency  $2\omega$ . In this goal, we postulate the formula

$$\ln p(t) \approx A + B\tau^\alpha + C\tau^\alpha \cos[\omega \ln(\tau) + \phi_1] + D\tau^\alpha \cos[2\omega \ln(\tau) + \phi_2] , \quad (16)$$

which differs from equation (1) by the addition of the last term proportional to the amplitude  $D$ . This formula has two additional parameters compared with (1), the amplitude  $D$  of the harmonic and its phase  $\phi_2$ . We follow the fit procedure of Ref. [31] with minor modifications, which itself adapts the slaving method of [8, 9]. By rewriting Eq. (16) as  $\ln p(t) = A + Bf(t) + Cg(t) + Dh(t)$ ,

we obtain a system of 4 linear equations for the four variables  $A$ ,  $B$ ,  $C$  and  $D$ :

$$\begin{pmatrix} \sum \ln p_i \\ \sum (\ln p_i) f_i \\ \sum (\ln p_i) g_i \\ \sum (\ln p_i) h_i \end{pmatrix} = \begin{pmatrix} N & \sum f_i & \sum g_i & \sum h_i \\ \sum f_i & \sum f_i^2 & \sum g_i f_i & \sum h_i f_i \\ \sum g_i & \sum f_i g_i & \sum g_i^2 & \sum h_i g_i \\ \sum h_i & \sum f_i h_i & \sum g_i h_i & \sum h_i^2 \end{pmatrix} \cdot \begin{pmatrix} A \\ B \\ C \\ D \end{pmatrix}, \quad (17)$$

where  $p_i = p(t_i)$ ,  $f_i = f(t_i)$ ,  $g_i = g(t_i)$  and  $h_i = h(t_i)$ . Solving analytically this system allows us to slave the four parameters  $A$ ,  $B$ ,  $C$  and  $D$  to the other parameters in the search for the best fit. With this approach, we find that the search of the optimal parameters is very stable and provides fits of very good quality in spite of the remaining five free parameters.

The results are listed in Table 2 and depicted in figure 10. The fit residuals are reduced considerably compared with the fits reported in Table 1. The improvement of the fits are obvious when comparing Fig. 10 with figure 2. Note also that  $|D| < |C|$  ( $|C| \approx 5|D|$ ) which is in agreement with the fact that the spectral peak of the fundamental log-frequency is much higher than the peak of the second harmonic approximately by a factor 5, as shown in Fig. 4 and Fig. 7.

We have also tested whether the addition of a third log-frequency around  $f \approx 2.8$  (which is not a third harmonic), as suggested from the spectral Lomb analyses shown in figures 4 and 7), could improve and/or modify the fit. We found a slight but non-significant reduction of the root-mean-square error with negligible modification of the fit, suggesting that this log-frequency is due to noise.

Since expression (16) contains the formula (1) as a special case  $D = 0$ , we can use Wilk's theorem [18] and the statistical methodology of nested hypotheses to assess whether the hypothesis that  $D = 0$  can be rejected. Therefore, the null hypothesis and its alternative are

1.  $H_0: D = 0$ ;
2.  $H_1: D \neq 0$ ;

The method proceeds as follows. By assuming a Gaussian distribution of observation errors (residuals) at each data point, the maximum likelihood estimation of the parameters amounts exactly to the minimization of the sum of the square over all data points (of number  $n$ ) of the differences  $\delta_j(i)$  between the mathematical formula and the data [17]. The standard deviation  $\sigma_j$  with  $j = 0, 1$  of the fits to the data associated respectively with (1) and (16) is given by  $1/n$  times the sum of the squares over all data points of the differences  $\delta_j^{(o)}(i)$  between the mathematical formula and the data, estimated for the optimal parameters of the fit. The log-likelihoods corresponding to the two hypotheses are thus given by

$$L_j = -n \ln \sqrt{2\pi} - n \ln \sigma_j - n/2, \quad (18)$$

where the third term results from the product of Gaussians in the likelihood, which is of the form

$$\propto \prod_{i=1}^n \exp[-(\delta_j^{(o)}(i))^2 / 2\sigma_j^2] = \exp[-n/2],$$

from the definition  $\sigma_j^2 = (1/n) \sum_{i=1}^n [\delta_j^{(o)}(i)]^2$ . Then, according to Wilk theorem of nested hypotheses, the log-likelihood-ratio

$$T = -2(L_0 - L_1) = 2n(\ln \sigma_1 - \ln \sigma_0), \quad (19)$$

is a chi-square variable with  $k$  degrees of freedom, where  $k$  is the number of restricted parameters [5]. In the present case, we have  $k = 1$ .

The Wilk test thus amounts to calculate the probability that the obtained value of  $T$  can be overpassed by chance alone. If this probability is small, this means that chance is not a convincing explanation for the large value of  $T$  which becomes meaningful. This implies a rejection of the hypothesis that  $D = 0$  is sufficient to explain the data and favor the fit with  $D \neq 0$  as statistically significant.

In our test, the beginning of the fitted data set is fixed at 09-Aug-2000, while the end of the data set varies from 01-Jan-2001 to 24-Aug-2002. The results of the Wilk test are presented in Table 3. Increasing the number of points decreases the probability that the obtained probability to overpass  $T$  may result from chance, and thus increases the statistical significance of the fit with Eq. (16). Since the assumption of Gaussian noise is most probably an under-estimation of the real distribution of noise amplitudes, the very significant improvement in the quality of the fit brought by the use of Eq. (16) quantified in Table 3 provides most probably a lower bound for the statistical significance of the hypothesis that  $D$  should be chosen non-zero, above the 99.8% confidence level. Indeed, a non-Gaussian noise with a fat-tailed distribution would be expected to decrease the relevance of competing formulas, whose performance could be scrambled and be made fuzzy. The clear and strong result of the Wilk test with assumed Gaussian noises thus confirm a very strong significance of Eq. (16).

Strengthened by this analysis of the strong relevance of the second harmonics at  $2\omega$ , we revisit the Nikkei index and fit it in the first 2.6 years of its decay starting in January 1990 using (16) to test whether the second harmonics is also important for the Nikkei index. The fit is compared with the log-price in Fig. 11. We find indeed an impressive improvement, as the mean square error  $\chi = 0.0457$  is significantly smaller than the mean square error  $\chi = 0.0535$  obtained with expression (1) and whose fit is shown in Fig. 1.

### 3 Discussion and prediction

Starting from a visual analogy with the Nikkei index shifted by 11 years, the first point of the analyses presented above is to have established with strong significance the existence of an anti-bubble followed by the S&P500 index approximately since July-August 2000. This anti-bubble is characterized by an overall power law decay of the index decorated by strong log-periodic oscillations.

Following the analogy with the trajectory of the Nikkei index 11 years earlier, the second point is that a comparison between the fits obtained with equations (1) and (3) shows that the S&P500 index has not yet entered into the second phase in which the angular log-frequency may start its shift to another value, as did the Nikkei index after about 2.5 years of its decay. We may expect this to occur in the future. Not being able to estimate directly the parameter  $\Delta_t$  controlling this transition due to the smallness of the S&P500 index anti-bubble duration, we can however offer the following guess, based on the hypothesis that the values  $\Delta_t$  and  $\Delta_\omega$  given by the fit of expression (3) to the logarithm of the Nikkei index are reasonable estimates of those for the S&P500 index. We use also the parameters in the column of  $t_{\text{start}} = \text{Aug-01-2000}$  of Table 1 for the first order regime and extrapolate the fitted curve to 2006 (continuous line). Using the values of the fits with (1) and plugging in the values of  $\Delta_t$  and  $\Delta_\omega$  from the Nikkei index in expression (3) gives the dashed line shown in Fig. 12. The crossover from the first order regime to the second order regime is here suggested to occur in the first half of 2004. Fig. 12 also compares the first-order fit and the second-order guess with formula (16) taking into account the second harmonics. Fig. 12 suggests

that the next broad minimum of the S&P500 index will occur in the first semester of 2004. This is consistent with the prediction (13) using Shank's transformation.

The third important point is the improvement in the quality of the fits and therefore in the potential for predictions when adding the harmonics at  $2\omega$ , as shown in figure 10 compared with figure 2. Figure 2 suggests a local maximum of the S&P500 index around the end of the first quarter of 2003, while figure 10 refines this prediction by seeing an earlier peak before but close to the end of 2002. These two predictions are not in contradiction: the prediction of figure 10 shows that the oscillatory structure of S&P500 index implies several ups and downs in the coming year, with a tendency to appreciate for a while before going down again by the end of 2003.

Ideally, we would like to combine the effect of the second-order formula (3) with the impact of the second harmonics described by expression (16). We do this by adding to (16) a term with the same structure as the one proportional to  $C_2$  in (3) with  $\omega$  replaced by  $2\omega$ , again fixing  $\Delta_t$  and  $\Delta_\omega$  at the values determined from the Nikkei index. Figure 13 compares the result of this fit with that with (16) and their extrapolation up to close to the end of 2006. These two curves provide a sense of the future directions of the S&P500 index and their probable degree of variability.

## 4 Concluding remarks

The growing awareness in 2002 of the crisis in the American financial system is reminiscent of the starting point of Japan's massive financial bubble burst more than 10 years before and of the intertwining of the bad debts and bad performance of banks whose capital is invested in the shares of other banks, thus creating the potential for a catastrophic cascade of bankrupts. Japan has rediscovered before the US the faults of the 19th century financial system in the US in which stock markets were so much intertwined with their overall banking financial system, that busts and bursts occurred more than once every decade, with firms losing their credit lines and workers and consumers their savings and often their employment. It is often said that the 1930s depression was the last of the stock market and bank-induced economic collapses. The growing fuzziness between financial banking systems and stock markets, in part due to the innovations in information technology, has re-created the climate for stronger bubbles and more pronounced losses of confidence leading to long-lived bearish regimes possibly nucleating depressions.

A big problem is that, in the collapse following them, policy interventions such as lowering interest rates, reducing taxes, government spending packages and any measure to restore investors' confidence may be much less effective, as discovered with the Japanese so-called liquidity trap, a process in which government and the central bank policy becomes essentially useless. In addition, loss of confidence by investors (for instance following the frauds in accounting in the US) may lead to a non-negligible cost to the overall economy [4], providing a positive feedback reinforcing the bearish climate.

We have proposed that the trajectories of the US and Japanese stock markets could be understood in large part by taking into account imitative and herding mechanisms, both stemming possibly from rational or irrational behaviors. A key ingredient entering probably in the imitative and herding processes is the phenomenon of investor confidence. It has recently been argued [24] that investor confidence can be understood far better if one assumes not that investors have rational expectations, but that they have what economists call "adaptive expectations." Individuals with rational expectations predict others' behavior by focusing on their external incentives and constraints. In contrast, individuals with adaptive expectations predict others' behavior (including possibly the behavior of such an abstract "other" as the stock market) by extrapolating from the past. In addi-

tion, confidence and trust in the market have been shown to be subjected to history effects [24]. We believe that these behavioral traits provide fundamental roots underlying the validity of our analysis which, ultimately, can be viewed similarly as nothing but a (rather complex nonlinear) extrapolation of the past.

Our theory does not describe the common “stationary” evolution of the stock market, but rather is specifically tailored for identifying “monsters” or anomalies (bubbles and their end) and for classifying their agonies. We claim that these agonies (the anti-bubbles) are mostly shaped by collective effects between economic and stock market agents, with their imitation and confidence (and lack thereof) idiosyncracies. Ultimately, our description must leave place to a recovery of the fundamental pricing principles (and of possible emergences of new speculative bubbles) but, before this, it describes the way by which collective effects control in large part the processes towards this recovery.

The present study complements and makes more precise a previous one focusing at longer times scales, based on three pieces of evidence, namely the growth over long time scales of population, gross national product and stock market indices [14, 20], which issued a prediction that starting around 1999, a 5 to 10 years consolidation of international stock markets will occur, allowing a purge after the over-aggressive appetite of the preceding decade. For more than the last two years, this prediction has been born out. The present study confirms this impression that the US stock market is not yet on the verge of recovery.

With its extraordinary and unparalleled growth, its ensuing decade-long absence of growth, its crowded land, its aging population, is Japan a precursor of the new regime that mankind has to shift to, as discussed in [14, 20]? It seems that the present qualification of the US market to be in an anti-bubble phase is entirely in line with these predictions. From a larger perspective and at the horizon of the end of the first half of this century, the behavior of these stock markets raise the following question: shall we learn the lessons of previous bubbles and crashes/depressions and shall we be able to transit to a qualitatively different organization of economic and cultural exchanges before the fundamental limitations of a finite earth and limited human intelligence set in?

**Acknowledgments:** We acknowledge stimulating discussions with D. Darcet and thank him for pointing out the similarity between the Nikkei and the S&P500 with a time-shift of about 11 years. We thank D. Stauffer for critical comments on the manuscript. This work was partially supported by NSF-DMR99-71475 and the James S. Mc Donnell Foundation 21st century scientist award/studying complex system.

## References

- [1] Bender C, Orszag S.A., *Advanced Mathematical Methods for Scientists and Engineers*. McGraw-Hill, New York (1978), page 147.
- [2] A. Erzan, Finite q-differences and the discrete renormalization group, *Phys. Lett. A* 225, 235-238 (1997).
- [3] Erzan, A. and J.P. Eckmann, q-analysis of Fractal Sets, *Phys. Rev. Lett.* 87, 3245-3248 (1997).
- [4] C. Graham, R. Litan and S. Sukhtanker, *Cooking the Books: The Cost to the Economy*, Brookings Policy Brief 106, 02/08 (2002) ([http : //www.brookings.edu/comm/policybriefs/pb106.htm](http://www.brookings.edu/comm/policybriefs/pb106.htm)).
- [5] Holden K, Peel DA and Thompson JL, *Economic Forecasting: An Introduction* (Cambridge University Press, Cambridge, 1990) pp.59.
- [6] Huang, Y., A. Johansen, M.W. Lee, H. Saleur and D. Sornette, Artifactual log-periodicity in finite size data: Relevance for earthquake aftershocks, *J. Geophys. Res.* 105, 25451-25471 (2000).
- [7] K. Ide and D. Sornette, Oscillatory Finite-Time Singularities in Finance, Population and Rupture, *Physica A* 307 (1-2), 63-106 (2002)
- [8] A. Johansen, D. Sornette and O. Ledoit, Predicting financial crashes using discrete scale invariance, *Journal of Risk* 1, 5-32 (1999).
- [9] A. Johansen, O. Ledoit and D. Sornette, Crashes as critical points, *International Journal of Theoretical and Applied Finance* Vol. 3, No. 2 219-255 (2000).
- [10] A. Johansen and D. Sornette, Critical Crashes, *Risk*, Vol 12, No. 1, p.91-94 (1999).
- [11] A. Johansen and D. Sornette, Financial “anti-bubbles”: Log-periodicity in Gold and Nikkei collapses, *Int. J. Mod. Phys. C* 10(4), 563-575 (1999).
- [12] A. Johansen and D. Sornette, Evaluation of the quantitative prediction of a trend reversal on the Japanese stock market in 1999, *Int. J. Mod. Phys. C* Vol. 11 (2), 359-364 (2000).
- [13] A. Johansen and D. Sornette, The Nasdaq crash of April 2000: Yet another example of log-periodicity in a speculative bubble ending in a crash, *European Physical Journal B* 17, 319-328 (2000).
- [14] A. Johansen and D. Sornette, Finite-time singularity in the dynamics of the world population and economic indices, *Physica A* 294 (3-4), 465-502 (2001).
- [15] A. Johansen, D. Sornette and A.E. Hansen, Punctuated vortex coalescence and discrete scale invariance in two-dimensional turbulence, *Physica D* 138, 302-315 (2000).
- [16] A. Johansen, D. Sornette and O. Ledoit, Predicting Financial Crashes using discrete scale invariance, *Journal of Risk* 1 (4), 5-32 (1999)
- [17] Press, W., S. Teukolsky, W. Vetterling and B. Flannery, *Numerical Recipes in FORTRAN: The Art of Scientific Computing* (Cambridge University, Cambridge, 1996).

- [18] Rao C, Linear statistical Inference and Its Applications (New York, Wiley, 1965) ch 6, section 6e.3.
- [19] D. Sornette, Discrete scale invariance and complex dimensions, Physics Reports 297, 239-270 (1998).
- [20] D. Sornette, Why Stock Markets Crash (Critical Events in Complex Financial Systems), Princeton University Press, Princeton, NJ, 2002, in press.
- [21] D. Sornette and A. Johansen, Large financial crashes, Physica A 245, N3-4, 411-422 (1997).
- [22] D. Sornette and A. Johansen, Significance of log-periodic precursors to financial crashes, Quantitative Finance 1, 452-471 (2001).
- [23] D. Sornette, A. Johansen and J.-P. Bouchaud, Stock market crashes, Precursors and Replicas, J.Phys.I France 6, 167-175 (1996)
- [24] L.A. Stout, The Investor Confidence Game, working paper available [http://papers.ssrn.com/paper.taf?abstract\\_id=322301](http://papers.ssrn.com/paper.taf?abstract_id=322301)
- [25] Wilson, K.G., Problems in Physics with many scales of length, Scientific American 241 (2), 158-179 (1979).
- [26] W.-X. Zhou and D. Sornette, Statistical significance of periodicity and log-periodicity with heavy-tailed correlated noise, Int. J. Mod. Phys. C 13 (2), 137-170 (2002).
- [27] W.-X. Zhou and D. Sornette, Evidence of Intermittent Cascades from Discrete Hierarchical Dissipation in Turbulence, Physica D 165, 94-125 (2002).
- [28] W.-X. Zhou and D. Sornette, Generalized q-Analysis of Log-Periodicity: Applications to Critical Ruptures, Phys. Rev. E, in press, <http://arXiv.org/abs/cond-mat/0201458>.
- [29] W.-X. Zhou and D. Sornette, Non-Parametric Analyses of Log-Periodic Precursors to Financial Crashes, preprint, <http://arXiv.org/abs/cond-mat/0205531>.
- [30] W.-X. Zhou, D. Sornette and V. Pisarenko, New Evidence of Discrete Scale Invariance in the Energy Dissipation of Three-Dimensional Turbulence: Correlation Approach and Direct Spectral Detection, submitted to Physical Review E (2002). (<http://arXiv.org/abs/cond-mat/0208347>)
- [31] W.-X. Zhou and D. Sornette, Positive Hazard Rate and Log-Periodicity, in preparation.

Table 1: Fitted parameters using equations (1) and (3) on the S&P500 index. The parameters with subscript 0 correspond to fits using equation (1) together with (2). The subscripts 1 and 2 refer to fits with expressions (1) and (3) respectively together with (4). The rows of  $\chi_0$ ,  $\chi_1$  and  $\chi_2$  present the standard deviations (r.m.s.) of the residuals for different fits. Note that the fits with the first-order formula (1) with definition (2) are unstable and sensitive to  $t_{\text{start}}$ . Comparing parameters with subscripts 1 and 2, one can see that applying (4) improves significantly the quality of the fits. With this new symmetric definition (4), we find that the first-order fits using (1) are quite robust and close to the fits with the second-order formula (3). The **bold** values are discussed in the text.

$t_{\text{start}}$	01/03	01/04	<b>01/05</b>	<b>01/06</b>	<b>01/07</b>	<b>01/08</b>	<b>01/09</b>	01/10	01/11	01/12
$t_{c,0}$	02/28	01/24	04/05	03/16	06/21	07/19	08/15	07/16	08/13	09/12
$t_{c,1}$	07/12	07/18	<b>08/06</b>	<b>08/06</b>	<b>08/06</b>	<b>08/18</b>	<b>08/10</b>	08/10	08/17	09/18
$t_{c,2}$	07/13	07/19	08/05	08/06	08/13	08/18	08/11	08/10	08/15	09/15
$\chi_0 \times 100$	3.969	3.790	3.752	3.605	3.423	3.303	3.277	3.363	3.369	3.406
$\chi_1 \times 100$	3.431	3.317	<b>3.187</b>	<b>3.217</b>	<b>3.229</b>	<b>3.218</b>	<b>3.277</b>	3.307	3.370	3.407
$\chi_2 \times 100$	3.415	3.315	3.182	3.215	3.209	3.218	3.276	3.307	3.370	3.407
$\alpha_0$	1.00	1.00	1.00	0.83	0.71	0.67	0.67	0.70	0.75	0.76
$\alpha_1$	0.80	0.74	<b>0.71</b>	<b>0.70</b>	<b>0.69</b>	<b>0.68</b>	<b>0.66</b>	0.73	0.75	0.77
$\alpha_2$	0.76	0.76	0.70	0.70	0.68	0.68	0.66	0.73	0.75	0.76
$\omega_0$	14.23	15.32	13.12	13.77	12.09	11.00	10.12	11.20	10.19	9.37
$\omega_1$	10.79	11.01	<b>10.30</b>	<b>10.35</b>	<b>10.50</b>	<b>10.04</b>	10.31	10.30	10.06	9.17
$\omega_2$	11.33	10.82	10.37	10.38	10.22	10.03	10.27	10.29	10.11	9.29
$\phi_0$	3.49	4.99	2.03	0.59	4.16	5.34	5.17	4.01	1.55	4.09
$\phi_1$	0.15	2.10	3.78	3.46	5.74	5.72	3.86	3.91	5.53	2.29
$\phi_2$	6.28	3.31	3.34	3.27	1.35	5.80	4.12	3.97	2.03	4.67
$A_1$	7.33	7.33	7.33	7.33	7.33	7.32	7.34	7.31	7.30	7.27
$A_2$	7.33	7.33	7.33	7.33	7.33	7.32	7.33	7.31	7.30	7.28
$B_1 \times 1000$	-2.10	-3.10	-4.10	-4.20	-4.38	-4.92	-5.66	-3.40	-2.78	-2.41
$B_2 \times 1000$	-2.85	-2.87	-4.23	-4.27	-4.88	-4.89	-5.50	-3.37	-2.78	-2.54
$C_1 \times 1000$	0.47	-0.68	0.92	0.94	-0.99	1.13	1.25	0.82	0.70	-0.67
$C_2 \times 1000$	-0.62	-0.64	0.94	0.95	-1.10	1.13	1.22	0.81	-0.70	0.70
$\Delta t$	12128	24032	35135	93922	64998	94620	100000	97552	94581	98337
$\Delta \omega$	0.00	4.92	6.04	8.39	0.11	2.79	0.00	0.00	0.26	9.98

Table 2: Parameters of the fit with equation (16) with (4) of the S&P500 index for different  $t_{\text{start}}$ . The fit residuals are strongly reduced compared with the fits shown in Table 1. The **bold** columns correspond to the values of  $t_{\text{start}}$  giving basically the same values for  $t_c, \alpha$  and  $\omega$ .

$t_{\text{start}}$	01/03	01/04	01/05	<b>01/06</b>	<b>01/07</b>	<b>01/08</b>	bf01/09	01/10	01/11	01/12
$t_c$	06/15	07/15	07/16	08/04	08/12	08/21	08/04	06/14	08/10	06/04
$\chi \times 100$	3.009	2.858	2.713	2.711	2.680	2.690	2.661	2.700	2.712	2.687
$\alpha$	0.79	0.68	0.65	0.65	0.61	0.61	0.54	0.60	0.57	0.57
$\omega$	12.12	11.56	11.77	10.70	10.74	10.26	10.97	12.24	10.86	12.49
$\phi_1$	3.88	5.01	3.76	1.41	1.39	4.52	2.89	6.28	0.59	1.35
$\phi_2$	4.90	0.66	4.39	2.98	2.80	2.84	5.83	0.24	1.20	2.88
$A$	7.33	7.34	7.34	7.34	7.34	7.33	7.38	7.39	7.35	7.40
$B \times 1000$	-2.19	-4.68	-5.59	-5.77	-7.60	-7.36	-12.42	-8.38	-10.34	-10.67
$C \times 1000$	0.44	-0.92	-1.09	1.21	1.54	1.58	-2.29	-1.44	2.03	1.79
$D \times 1000$	0.22	0.47	0.59	-0.53	-0.77	-0.71	-1.14	-0.77	-1.03	-0.96

Table 3: Likelihood-ratio test of the hypothesis that  $D \neq 0$  in Eq. (16). The beginning of the data set for fit is set to be fixed at 09-Aug-2000. The end of the data set varies from 01-Jan-2001 to 24-Aug-2002. The  $n$  column gives the number of the data set for each fit. The confidence level quantified by Proba decreases on average with  $n$ . There is no doubt that the  $H_1$  hypothesis of  $D \neq 0$  can not be rejected for all cases in the 99.8% confidence level.

$t_{\text{last}}$	$n$	$\sigma_1$	$\sigma_0$	$T$	Proba
01/01/01	101	0.0235	0.0283	18.7	0.0015%
01/31/01	121	0.0310	0.0381	24.8	$< 10^{-4}\%$
03/02/01	142	0.0341	0.0440	36.2	$< 10^{-4}\%$
04/01/01	163	0.0578	0.0616	10.3	0.13%
05/01/01	183	0.0831	0.0934	21.3	0.0004%
05/31/01	204	0.0949	0.1026	15.9	0.0067%
06/30/01	225	0.0984	0.1064	17.7	0.0026%
07/30/01	245	0.1022	0.1260	51.2	$< 10^{-4}\%$
08/29/01	267	0.1087	0.1544	93.9	$< 10^{-4}\%$
09/28/01	284	0.1332	0.1897	100.4	$< 10^{-4}\%$
10/28/01	305	0.1817	0.2181	55.7	$< 10^{-4}\%$
11/27/01	325	0.1855	0.2512	98.4	$< 10^{-4}\%$
12/27/01	346	0.1971	0.2552	89.4	$< 10^{-4}\%$
01/26/02	365	0.1987	0.2659	106.2	$< 10^{-4}\%$
02/25/02	385	0.2055	0.2895	132.0	$< 10^{-4}\%$
03/27/02	407	0.2329	0.3274	138.6	$< 10^{-4}\%$
04/26/02	428	0.2363	0.3353	149.7	$< 10^{-4}\%$
05/26/02	448	0.2482	0.3456	148.3	$< 10^{-4}\%$
06/25/02	469	0.2573	0.3515	146.4	$< 10^{-4}\%$
07/25/02	489	0.3170	0.4867	209.6	$< 10^{-4}\%$
08/24/02	510	0.3582	0.5339	203.6	$< 10^{-4}\%$

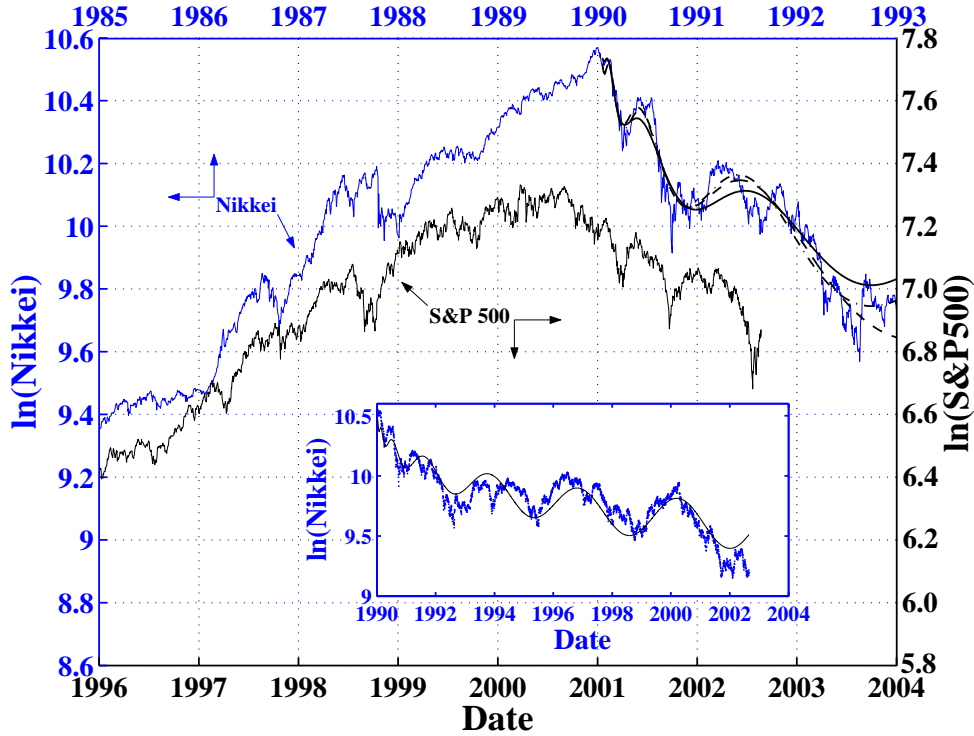


Figure 1: Comparison between the evolutions of the US S&P500 index from 1996 till August, 24, 2002 (bottom and right axes) and the Japanese Nikkei index from 1985 to 1993 (top and left axes). The years are written on the horizontal axis (and marked by a tick on the axis) where January 1 of that year occurs. The dashed line is the simple log-periodic formula (1) fitted to the Nikkei index. The data used in this fit goes from 01-Jan-1990 to 01-Jul-1992 [11]. The parameter values are  $t_c = 28\text{-Dec-1989}$ ,  $\alpha = 0.38$ ,  $\omega = 5.0$ ,  $\phi = 2.59$ ,  $A = 10.76$ ,  $B = -0.067$  and  $C = -0.011$ . The fit error is  $\chi = 0.0535$ . The dash-dotted line is the improved nonlinear log-periodic formula (3) developed in [21] fitted to the Nikkei index. The Nikkei index data used in this fit goes from 01-Jan-1990 to 01-Jul-1995 [11]. The parameter values are  $t_c = 27\text{-Dec-1989}$ ,  $\alpha = 0.38$ ,  $\omega = 4.8$ ,  $\phi = 6.27$ ,  $\Delta_t = 6954$ ,  $\Delta_\omega = 6.5$ ,  $A = 10.77$ ,  $B = -0.070$ ,  $C = 0.012$ . The fit error is  $\chi = 0.0603$ . The continuous line is the fit of the Nikkei index with the third-order formula developed in Ref. [11]. The Nikkei index data used in the fit goes from 01-Jan-1990 to 31-Dec-2000. The fit is performed by fixing  $t_c$ ,  $\alpha$  and  $\omega$  at the values obtained from the second-order fit and adjusting only  $\Delta_t$ ,  $\Delta'_t$ ,  $\Delta_\omega$ ,  $\Delta'_\omega$  and  $\phi$ . The parameter values are  $\Delta_t = 1696$ ,  $\Delta'_t = 5146$ ,  $\Delta_\omega = -1.7$ ,  $\Delta'_\omega = 40$ ,  $\phi = 6.27$ ,  $A = 10.86$ ,  $B = -0.090$ ,  $C = -0.0095$ . The fit error is  $\chi = 0.0867$ . In the three fits,  $A$ ,  $B$  and  $C$  are slaved to the other variables by multiplier approach in each iteration of optimization search. The inset shows the 13-year Nikkei anti-bubble with the fit with the third-order formula shown as the continuous line. The parameter values are  $\Delta_t = 52414$ ,  $\Delta'_t = 17425$ ,  $\Delta_\omega = 23.7$ ,  $\Delta'_\omega = 127.5$ ,  $\phi = 5.57$ ,  $A = 10.57$ ,  $B = -0.045$ ,  $C = 0.0087$ . The fit error is  $\chi = 0.1101$ . In all our fits, times are expressed in units of days, in contrast with the yearly unit used in [11]). Thus, the parameters  $B$  and  $C$  are different since they are unit-dependent, while all the other parameters are independent of the units.

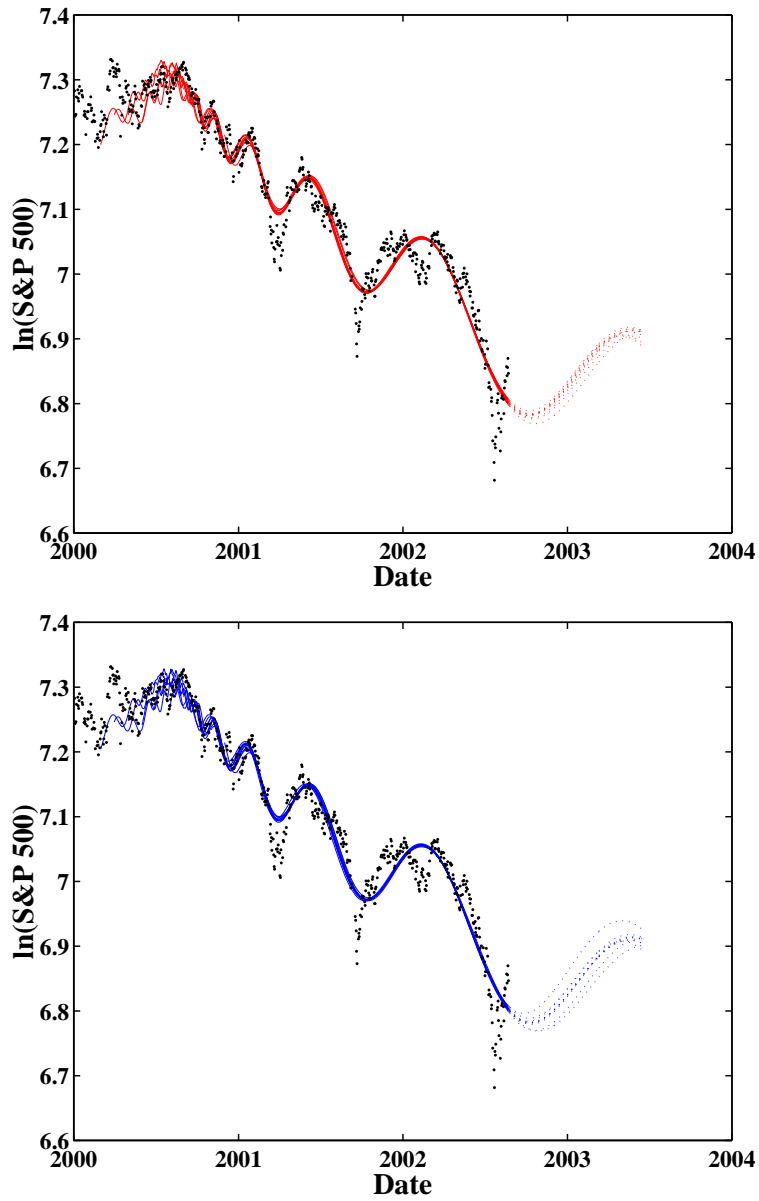


Figure 2: The S&P500 index anti-bubble fitted from  $t_{\text{start}}$  to August, 24, 2002, with the improved scheme (4) inserted in the two formulas (1) (upper panel) and (3) (lower panel) for different choices of  $t_{\text{start}}$ , spanning from Mar-01-2000 to Dec-01-2000. The dotted lines show the predicted future trajectories. One see that the fits are robust with respect to different starting date.

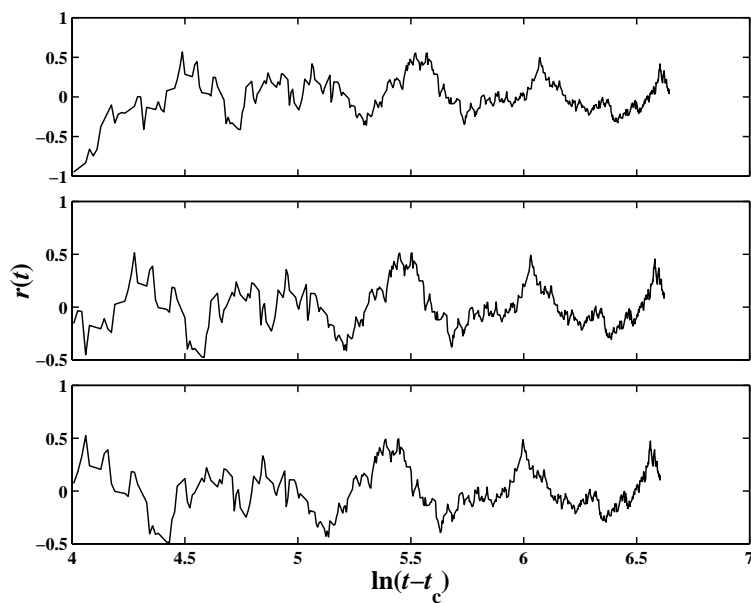


Figure 3: The residuals  $r(t)$  defined in Eq. (14) as a function of  $\ln(t - t_c)$ . The three plots from top to bottom correspond respectively to  $t_c = 15\text{-Jul-2000}$ ,  $t_c = 01\text{-Aug-2000}$  and  $t_c = 15\text{-Aug-2000}$ .

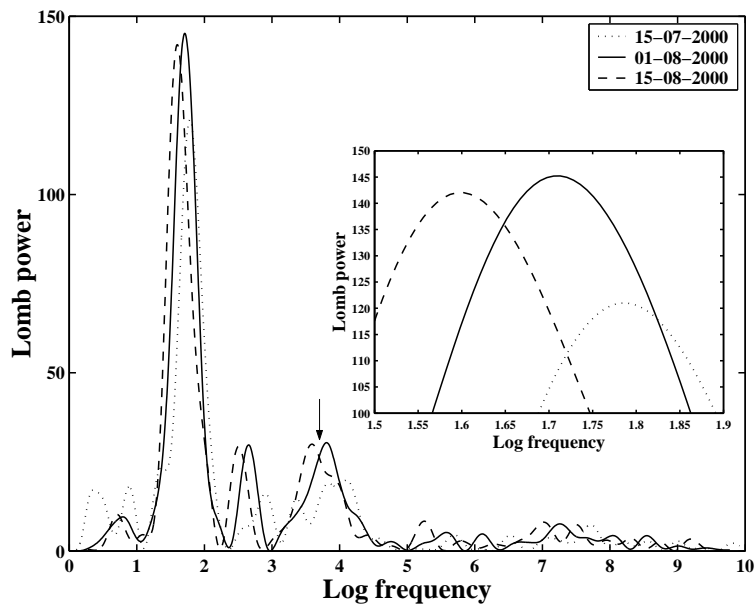


Figure 4: Lomb periodograms of the residuals  $r(t)$  shown in Fig. 3. The highest Lomb peaks are very significant. The second harmonics is also visible and is indicated by a downward pointing arrow. The inset shows a magnification of the Lomb periodogram in the neighborhood of the stronger peaks.

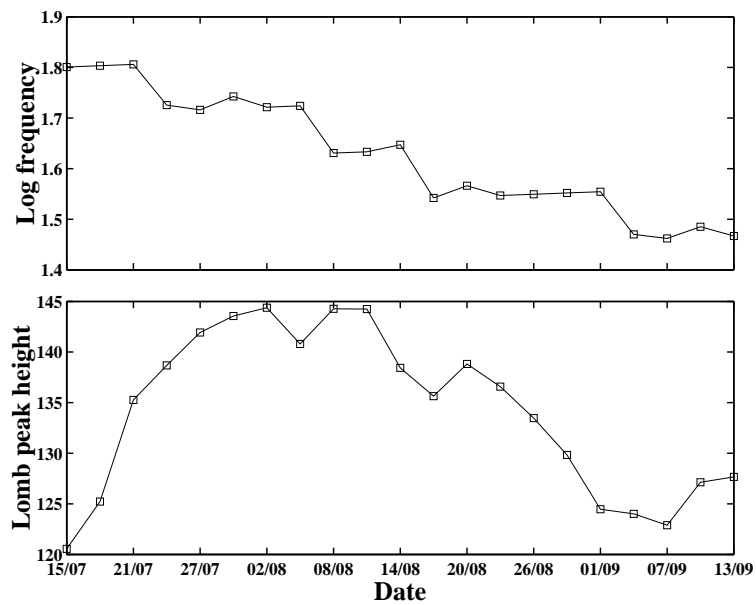


Figure 5: Amplitude of the highest Lomb peaks (lower panel) and their associated log-frequencies (upper panel) obtained by apply the parametric detrending approach of section 2.4.1 for 21 different critical  $t_c$  evenly spaced in the time interval from 15-Jul-2000 to 13-Sep-2000.

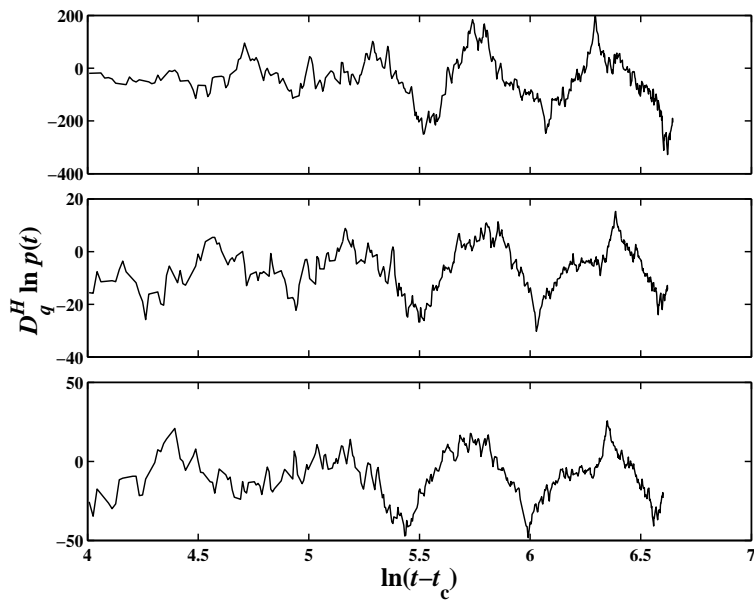


Figure 6: The  $(H, q)$ -derivatives of the logarithm of the S&P500 index as a function of  $\ln(t - t_c)$  for three value of  $t_c$ : 15-Jul-2000 with  $H = 0$  and  $q = 0.8$  in the top panel, 02-Aug-2000 with  $H = 0.5$  and  $q = 0.7$  in the mid panel, and 16-Aug-2000 with  $H = 0.4$  and  $q = 0.7$  in the bottom panel.

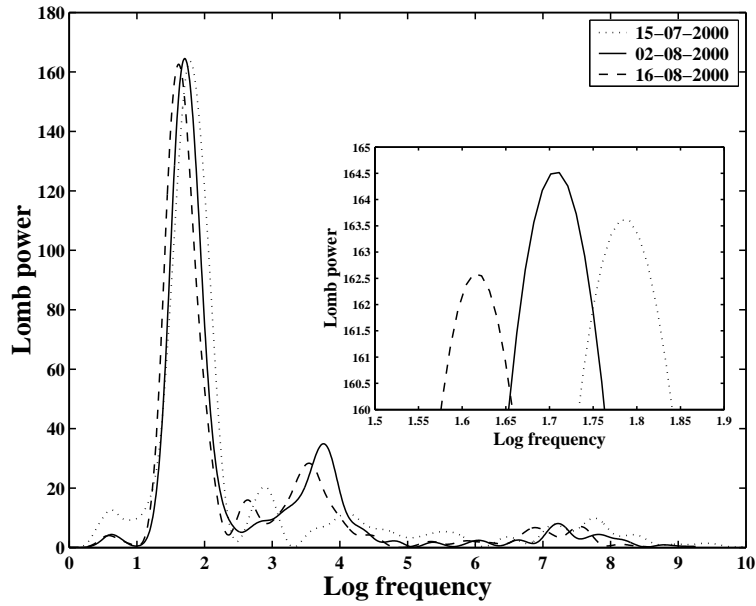


Figure 7: Lomb periodograms of the  $(H, q)$ -derivatives shown in Fig. 6 for three different value of  $t_c$ . The highest Lomb peaks are even more significant than those in Fig. 4. The inset shows the magnified Lomb peaks in the neighborhood of the maxima.

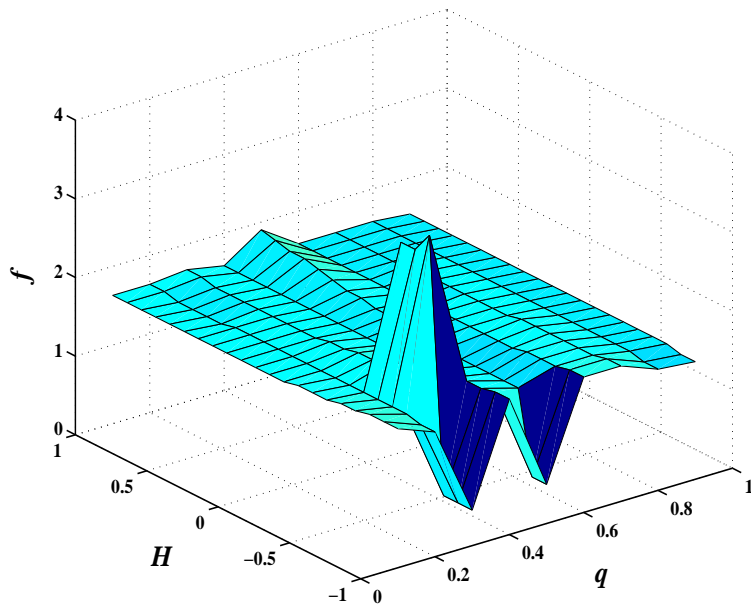


Figure 8: Log-frequency  $f$  as a function of  $H$  and  $q$  for  $t_c = 16\text{-Aug-2000}$ . The plateau at  $f = 1.62 \pm 0.07$  is a signature of the robustness of the detection of log-periodicity by the  $(H, q)$ -analysis.

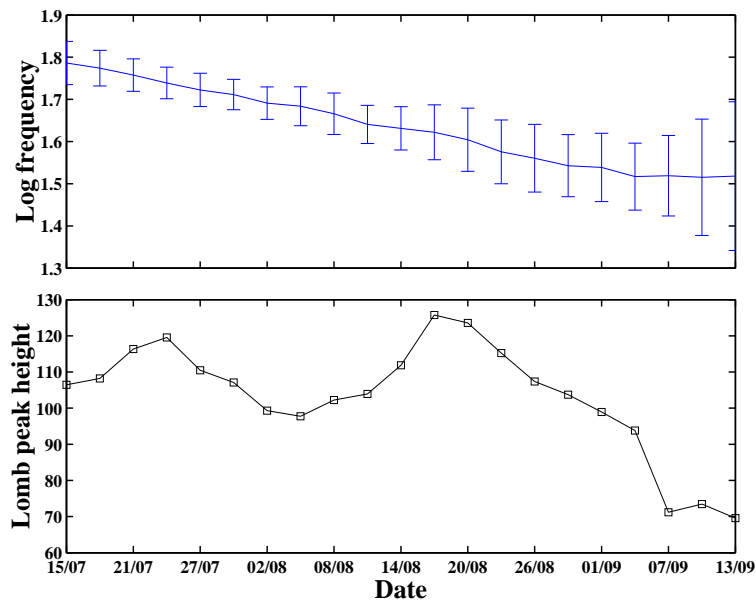


Figure 9: The highest Lomb peaks (lower panel) and their associated log-frequencies (upper panel) obtained by apply the non-parametric  $(H, q)$ -analysis for 21 different critical  $t_c$  evenly spaced shown as the abscissa. The Lomb peak height and the log-frequency are obtained by averaging all Lomb periodograms over all pairs  $(H, q)$  defined by scanning  $H$  from  $-1$  to  $1$  with spacing  $0.1$  and  $q$  from  $0.1$  to  $0.9$  with spacing  $0.1$ .

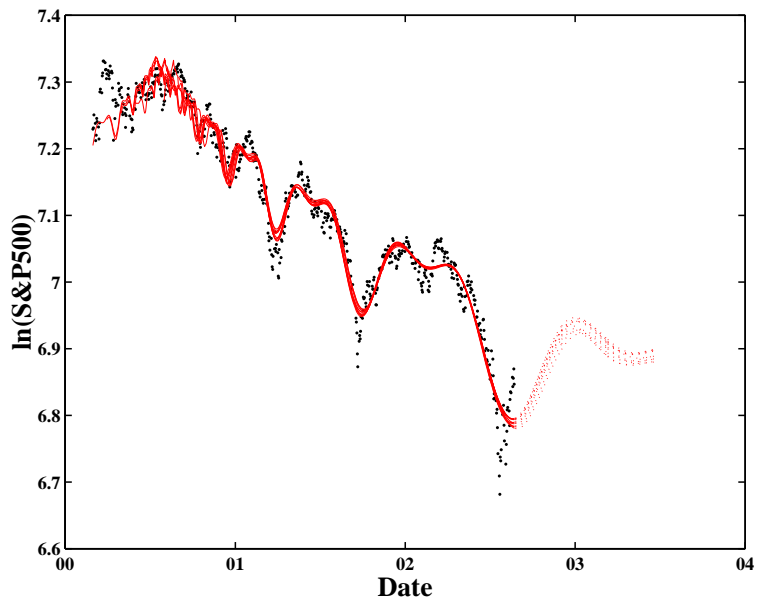


Figure 10: All the fitted functions using Eq. (16). The dotted lines show the predicted future trajectories. One sees that the fits are quite robust with respect to different starting date  $t_{\text{start}}$  from Mar-01-2000 to Dec-01-2000.

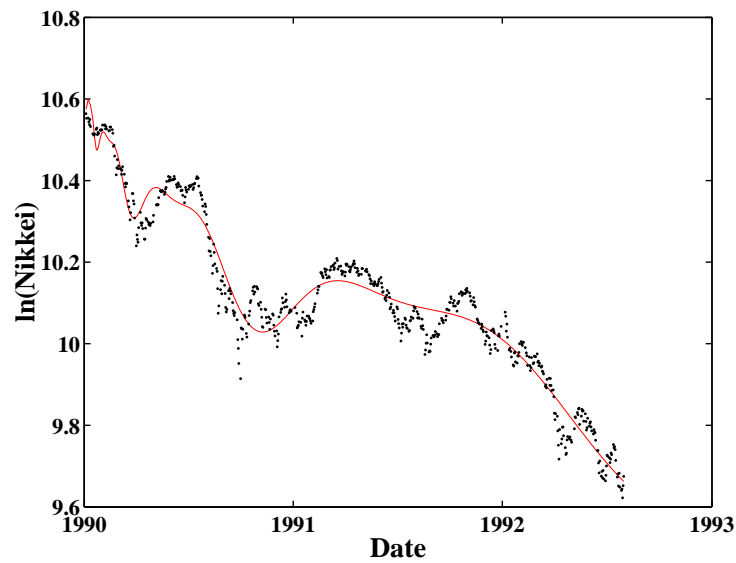


Figure 11: Fit of the 2.6 first years of the Nikkei index anti-bubble from Jan-01-1990 to Jul-31-1992 by Eq. (16) to test for the importance of a second harmonics. The parameter values are  $t_c = 27\text{-Dec-1989}$ ,  $\alpha = 0.42$ ,  $\omega = 5.1$ ,  $\phi_1 = 5.60$ ,  $\phi_2 = 1.80$ ,  $A = 10.72$ ,  $B = -0.051$ ,  $C = 0.0096$  and  $D = 0.0034$ . The r.m.s. error of this fit is  $\chi = 0.0457$ .

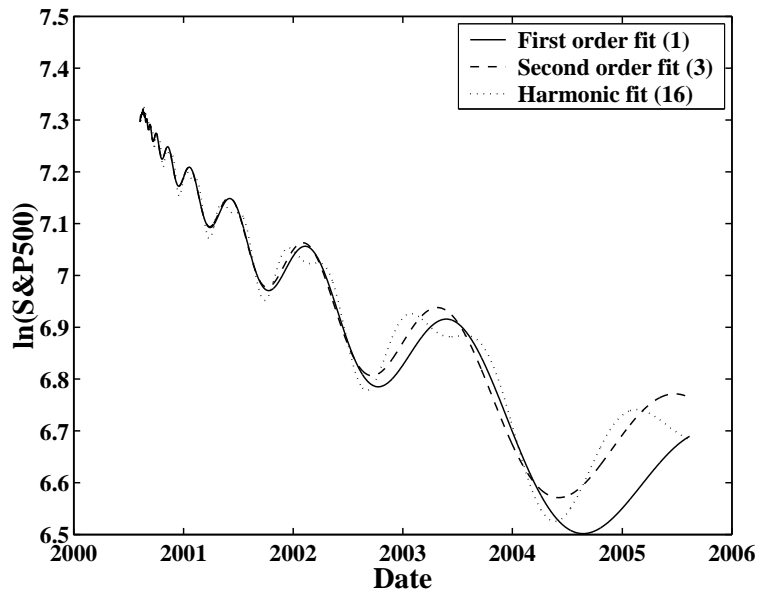


Figure 12: Prediction of a change of regime from the first order formula (1) to the second order formula (3). For the first order formula (1), we use the parameters corresponding to  $t_c = \text{Aug-01-2000}$  given in Table 1. The second order fit (3) uses the same parameter values as the first-order formula with the addition that  $\Delta_t$  and  $\Delta_\omega$  are fixed to the values determined the corresponding fit to the Nikkei index extending over 5 years of data. The crossover between the two formulas is predicted to occur in the first semester of 2004. We also show for comparison the fit using expression (16) taking into account the second harmonics at the angular log-frequency  $2\omega$ , with the parameters given in Table 2.

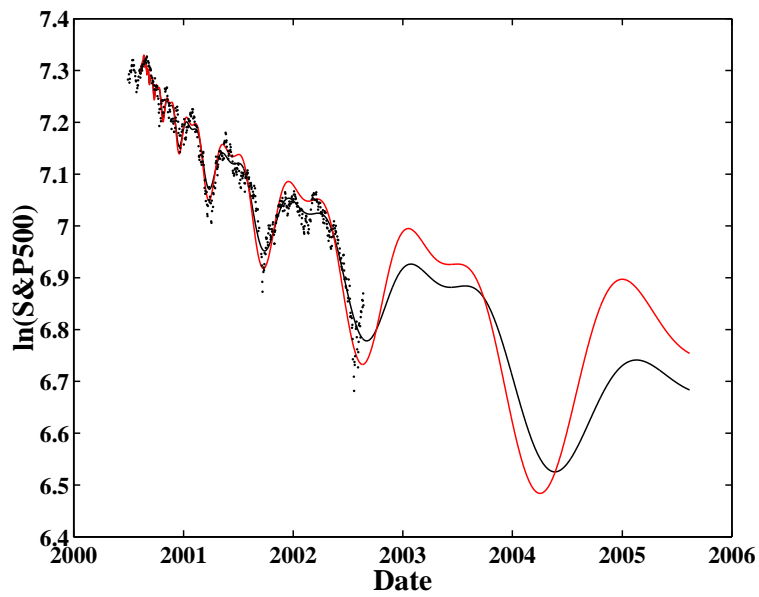


Figure 13: Combination of the effect of the second-order formula (3) with the impact of the second harmonics described by expression (16) (see text for explanations). The corresponding fit (thin continuous line) is compared with expression (16) (second harmonic effect only in thick continuous line) and extrapolates them up to close to the end of 2006.